

# Bacteriophage P2 and P4 Morphogenesis: Structure and Function of the Connector

Svein Rishovd,\*† Andreas Holzenburg,‡ Bjørn V. Johansen,†§ and Bjørn H. Lindqvist\*,<sup>1</sup>

\*Institute of Biology and The Biotechnology Centre of Oslo, University of Oslo, P.O. Box 1125, Blindern N-0317 Oslo, Norway;

†Electron Microscopy Unit for the Biological Sciences, Institute of Biology, University of Oslo, Oslo, Norway;

‡School of Biochemistry and Molecular Biology and School of Biology, University of Leeds LS2 9JT, United Kingdom; and §National Institute of Public Health, Oslo, Norway

Received April 3, 1997; returned to author for revision June 28, 1997; accepted March 17, 1998

The connector, the structure located between the bacteriophage capsid and tail, is interesting from several points of view. The connector is in many cases involved in the initiation of the capsid assembly process, functions as a gate for DNA transport in and out of the capsid, and is, as implied by the name, the structure connecting a tail to the capsid. Occupying a position on a 5-fold axis in the capsid and connected to a coaxial 6-fold tail, it mediates a symmetry mismatch between the two. To understand how the connector is capable of all these interactions its structure needs to be worked out. We have focused on the bacteriophage P2/P4 connector, and here we report an image reconstruction based on 2D crystalline layers of connector protein expressed from a plasmid in the absence of other phage proteins. The overall design of the connector complies well with that of other phage connectors, being a toroid structure having a conspicuous central channel. Our data suggests a 12-fold symmetry, i.e., 12 protrusions emerge from the more compact central part of the structure. However, rotational analysis of single particles suggests that there are both 12- and 13-mers present in the crude sample. The connectors used in this image reconstruction work differ from connectors in virions by having retained the amino-terminal 26 amino acids normally cleaved off during the morphogenetic process. We have used different late gene mutants to demonstrate that this processing occurs during DNA packaging, since only mutants in gene *P*, coding for the large terminase subunit, accumulate uncleaved connector protein. The suggestion that the cleavage might be intimately involved in the DNA packaging process is substantiated by the fact that the fragment cleaved off is highly basic and is homologous to known DNA binding sequences. © 1998 Academic Press

**Key Words:** bacteriophage; morphogenesis; P2; P4; connector.

## INTRODUCTION

Connectors are multifunctional structures involved in several processes during the bacteriophage life cycle. In many cases the connector is necessary for proper capsid assembly, probably by nucleating the assembly process. The structure is also essential for DNA packaging, possibly by constituting a gate for the dsDNA genome. After DNA packaging the capsid is connected to a tail by the connector, which thus mediates the symmetry mismatch between the fivefold capsid vertex and the sixfold tail. At the start of a new infectious cycle, the connector is involved in the ejection of DNA from the capsid into the host cell. As expected, the structure/function relationship of the connector has attracted considerable interest (reviewed in Bazinet and King, 1985; and Valpuesta and Carrascosa, 1994). Several phage connectors have been studied in great detail:  $\lambda$  (Kochan *et al.*, 1984), P22 (Bazinet *et al.*, 1988), T3 (Donate *et al.*, 1988; Valpuesta *et al.*, 1992), T4 (Driedonks *et al.*, 1981; Driedonks and Caldentey, 1983), T7 (Zachary and Black, 1992), phi29 (Carazo *et*

*al.*, 1985, 1986; Carrascosa *et al.*, 1985), and SPP1 (Dube *et al.*, 1993). We have concentrated on the connector of phage P2 for several reasons. First, both phage P2 and satellite phage P4 capsids (with triangulation numbers  $T = 7$  and  $T = 4$ , respectively), as well as procapsid analogs, have been reconstructed at high resolution from electron micrographs (Dokland *et al.*, 1992, 1993; Marvik *et al.*, 1995). Second, the gene coding for the connector protein of P2, gpQ, has been cloned, and the protein purified (Linderoth *et al.*, 1991; Rishovd *et al.*, 1994), opening the possibility of obtaining large amounts of the protein for structural studies. Third, biochemical and genetic evidence strongly indicated that the connector protein was cleaved at some point during the morphogenetic process (Rishovd *et al.*, 1994). The removal of 26 amino acids from the amino-terminal end decreases the calculated *pI* from 8.95 to 6.54, a value more in line with that of connector proteins of other phages. This suggests that a major structural change might be important in the control of the morphogenetic process. In this work we present an image reconstruction of the P2/P4 connector, and we identify the stage in the morphogenetic process at which the amino-terminal fragment of the connector protein is removed.

<sup>1</sup>To whom correspondence and reprint requests should be addressed.

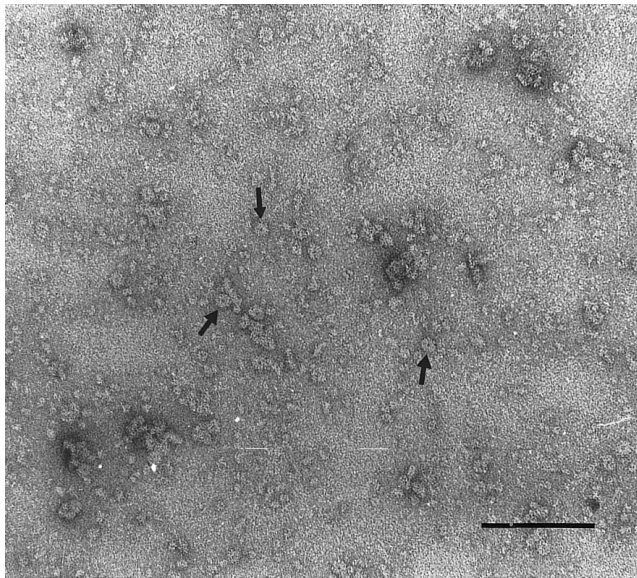


**FIG. 1.** Electron micrograph of negatively stained (protein appears white) gpQ-assembled single connectors. The arrows point at connectors in a typical face-on projection revealing a characteristic central depression. The scale bar corresponds to  $1\ \mu\text{m}$ .

## RESULTS

Previous work has shown that purified gpQ (the P2 connector protein), expressed from a plasmid, assembles into connector-like structures in the absence of other phage proteins (Rishovd *et al.*, 1994). Analogous observations have been reported for other bacteriophages (Ibanez *et al.*, 1984; Valpuesta *et al.*, 1992; Dube *et al.*, 1993). This finding suggests that the assembly of the connector may constitute a very early morphogenetic event. The single connectors observed in top view orientation in the electron microscope (see Fig. 1) are about  $135\ \text{\AA}$  in diameter and consist of the uncleaved connector protein only. They appear quite similar to other phage connectors, having lobes radiating from a central hub with a central channel. To obtain more detailed information 2D crystals were grown. An electron micrograph of a typical crystal, and its Fourier transform, is presented in Fig. 2. Compared to the single connectors in Fig. 1, the regularly spaced protein deficits in this crystal, interpreted as central channels, are only about  $80\ \text{\AA}$  apart, suggesting that this crystal-type is actually a thin 3D crystal comprising at least two layers that are not in register but offset by half a unit cell (see Fig. 3). This is also echoed in the diffraction pattern where the  $(h, k) = (1, 1)$  and  $(2, 0)$  reflections are much stronger than the  $(h, k) = (1, 0)$  reflection. The  $80\ \text{\AA}$  distance between the central channels in projection through at least two layers would then result in a periodicity of  $113\ \text{\AA}$  within a single layer (Fig. 3). Image processing resulted in a map (Fig. 4) that is in good agreement with this interpretation. However, projections through more than one layer have to be interpreted with care. Stain trapping and a nonuniform

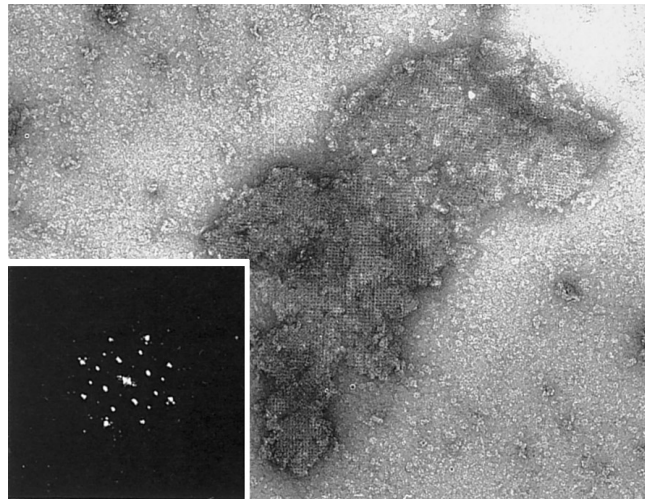


**FIG. 2.** Electron micrograph of a negatively stained thin 3D connector crystal (scale bar is  $1\ \mu\text{m}$ ), with the inset showing the corresponding diffraction pattern (scale 2:1, cf. Fig. 5).

stain distribution along the z-axis can result in the observed modulations in regions characterized by protein deficits. A very similar modulation is observed with thin 3D crystals of the enzyme d-ribulose-1,5-bisphosphate carboxylase/oxygenase (Holzenburg and Mayer, 1989). The fact that little structural information is obtained on the interesting peripheral parts of the connector—other than the four, orthogonally aligned, paired protrusions (arms) which appear to make the lateral contacts in the crystal lattice—could be ascribed to the same effect.

Crystals exhibiting a periodicity of  $113\ \text{\AA}$  were truly 2D ( $a = b = 113\ \text{\AA}$ ,  $\chi = 90^\circ$ , p4 plane group). A typical

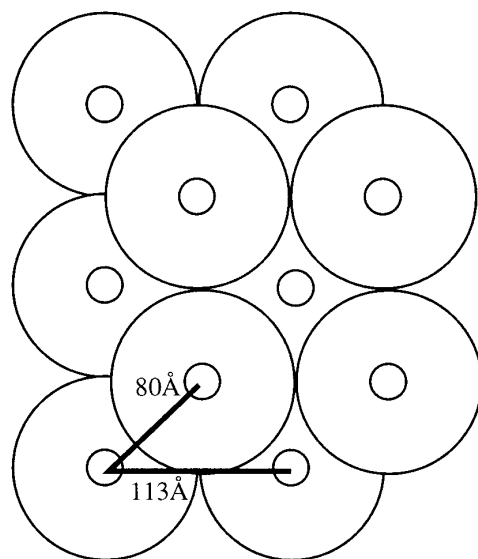


**FIG. 3.** Schematic representation of the organization of two displaced crystalline layers in a 3D connector crystal giving rise to stain traps with a periodicity of  $80\ \text{\AA}$ . Viewing direction is perpendicular to the (a,b)-plane.

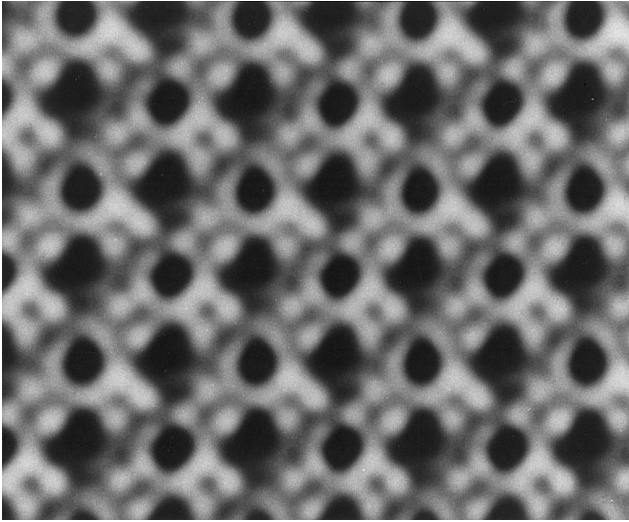


FIG. 4. Fourier projection map (calculated in p1) of connectors organized in thin 3D crystals (protein appears white). The horizontal center-to-center distance is 113 Å.

example, with its Fourier transform, is shown in Fig. 5. The projection map reveals a central channel (Fig. 6) of about 20 Å diameter which is very well defined by the surrounding domains. The periphery is delineated by protrusions. As evident from a visual inspection, two are directed toward each of the four neighboring connectors and another four at a 45° angle between the latter, suggesting a total of 12 protrusions. This finding was corroborated by an analysis of the rotational power spectra, which consistently showed strong peaks for fourfold symmetry. The p4-symmetrized projection map for the single layer is shown in Fig. 7. (When all three areas are merged in p1, the phase residual in p4 is 21.5.) In this interpretation the P2/P4 connector is a slightly handed structure.

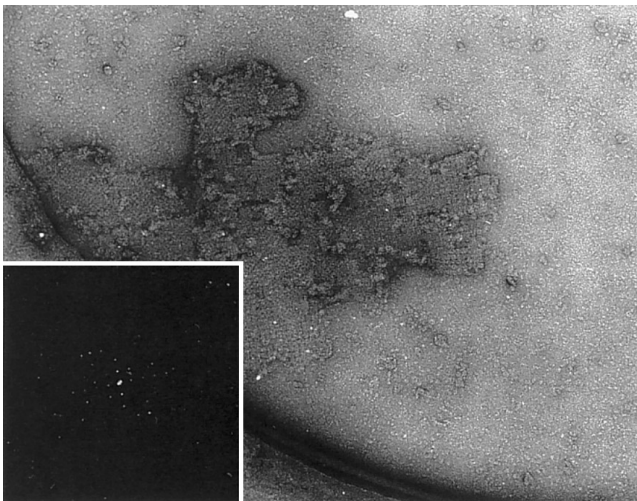


FIG. 5. Electron micrograph of a negatively stained 2D connector crystal (scale bar is 1 μm), with the inset showing the corresponding diffraction pattern (scale 1:1).

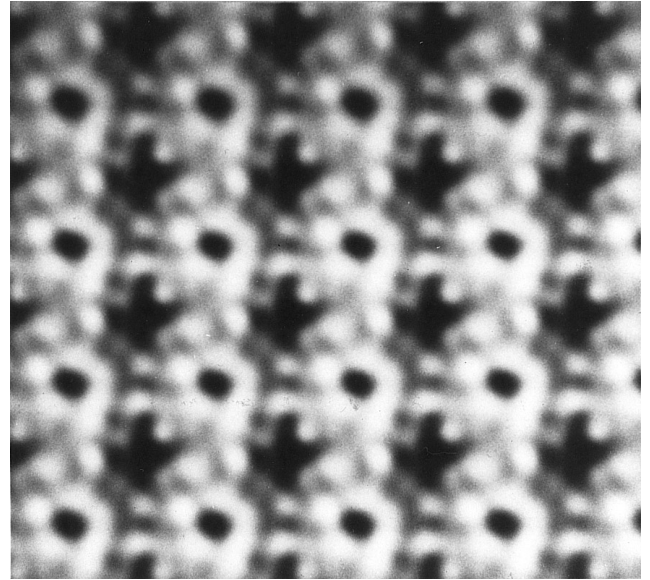


FIG. 6. Fourier projection maps (calculated in p1) of connectors organized in thin 2D crystals (protein appears white). The horizontal center-to-center distance is 113 Å.

As previously mentioned, the P2 connector is processed during the phage morphogenetic process. In the absence of capsids, no processing of gpQ occurs (for example an *amN<sub>209</sub>* mutant infection (Rishovd, 1993), or in the strain expressing gpQ from a plasmid (Rishovd *et al.*, 1994; Fig. 8, lane l)). Since no uncleaved gpQ is present in virions (Rishovd *et al.*, 1994; Fig. 8, lane k) the processing is presumed to be an essential part of the morphogenesis. To ascertain when the processing occurs we have infected various *Escherichia coli* strains harboring P2 late gene

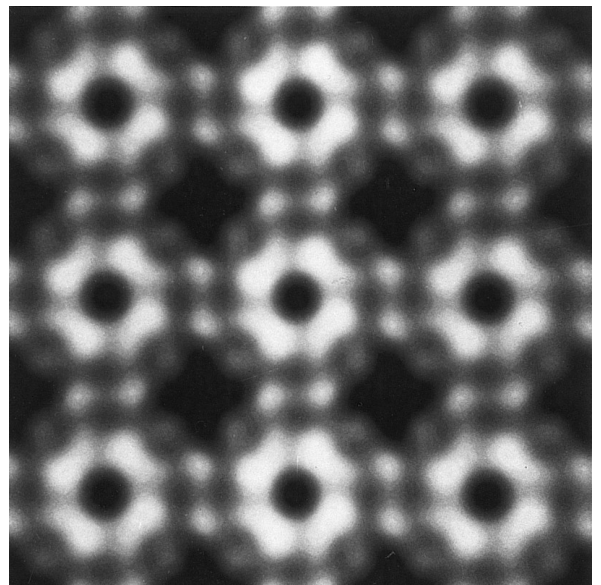
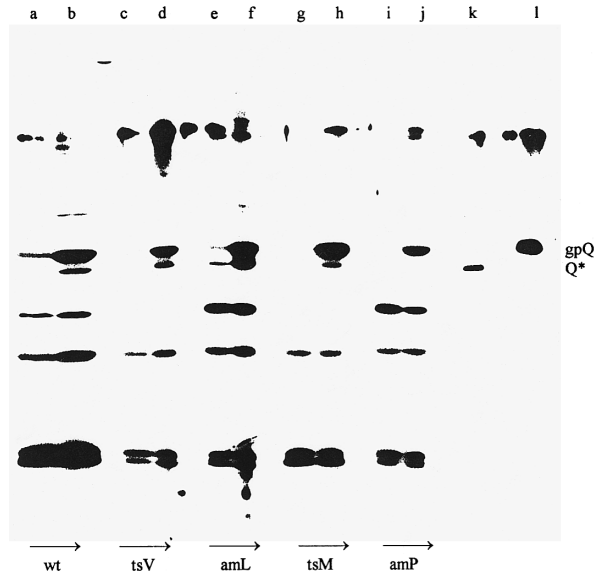


FIG. 7. Projection map of three single-layered areas merged, with p4 symmetry imposed. The horizontal center-to-center distance is 113 Å.



**FIG. 8.** Western blot of a 12% SDS-polyacrylamide gel showing the status of gpQ and Q\* in bacterial strains carrying different prophages when infected with P4vir1. The specific antiserum raised against gpQ has been described previously (Rishovd *et al.*, 1994). The samples are: C-1592 (harboring a "wild type" P2 prophage) 10 min (lane a) and 50 min (lane b) after infection; strain C-373 (harboring a P2tsV<sub>199</sub> prophage) 10 min (lane c) and 40 min (lane d) after infection; C-317 (harboring a P2amL<sub>9</sub> prophage) 20 min (lane e) and 55 min (lane f) after infection; C-1512 (harboring a P2tsM<sub>52</sub> prophage) 10 min (lane g) and 40 min (lane h) after infection; and C-322 (harboring a P2amP<sub>137</sub> prophage) 10 min (lane i) and 60 min (lane j) after infection. Lane k is P2vir1 phage particles purified on a CsCl gradient. Lane l is purified gpQ, as used in the crystallization experiments. The bands corresponding to gpQ and Q\* detected only when using the anti-Q serum, in contrast to the additional bands which are detected even with the secondary antibodies alone.

mutants as prophages with P4vir1. Infection experiments (see Materials and Methods) were performed under non-permissive conditions for the mutants, and the status of the connector protein was assayed with specific antibodies at the end of the morphogenetic process, i.e., just prior to lysis. Strain C-1592, harboring a P2cox3 prophage, is the common "wild type" host when growing P4 stocks (since it reduces the background of P2 phage). As shown in Fig. 8 lanes a and b, substantial amounts of the cleaved product, Q\*, is observed before lysis. The strain C-373 carries a prophage defective in the assembly of tails and is expected to accumulate capsids filled with DNA, being ready for the addition of tails. As in the wild-type situation, cleaved gpQ is indeed observed (Fig. 8, lanes c and d), demonstrating that gpQ is processed before the addition of a tail. The only known gene to act on the capsid in the interval between DNA packaging and the addition of a tail is gene *L* (Pruss and Calendar, 1978). C-317 carries an amber *L* P2 prophage, thus blocking the morphogenesis after DNA packaging. As demonstrated in Fig. 8 (lanes e and f) gpQ is cleaved when P4 infects this lysogen, implying that the cleavage reaction must take place some time prior to the

completion of DNA packaging. The terminase is responsible for DNA packaging. As in other phage systems the terminase is a multimeric complex, consisting of two subunits (gpM and gpP). Strain C-1512, containing a P2tsM<sub>52</sub> prophage defective in DNA packaging, infected with P4vir1, contains relatively small amounts of Q\* (Fig. 8, lanes g and h). This tendency toward less effective processing is more obvious in the *amP* situation. Strain C-322, lysogenic with an *amP*<sub>137</sub> prophage, infected with P4vir1, is effectively blocked in processing. Thus, processing of gpQ does not occur prior to the time gpP exerts its function, presumably in DNA packaging. In conclusion, gpP on its own or as a terminase subunit is directly or indirectly responsible for the processing of gpQ concomitant with DNA packaging.

## DISCUSSION

Our results on the structure of the P2/P4 connector suggest that it is very similar in overall design to the other phage connectors studied so far. Thus, in spite of any obvious sequence homology on the DNA/protein level (Black, 1988; Linderoth *et al.*, 1991), all connector proteins assemble into disc-like toroid structures having most of the density surrounding a central channel, with a number of protrusions along the periphery. The exact number of protrusions (monomers) per connector is a contentious issue. Different results have been reported according to the origin of the material and the context. Connectors in crystalline arrays have generally been described as 12-mers, whereas connectors observed as single particles, often assembled from protein expressed from plasmids, have also been described as 13-mers. Our suggestion that P2/P4 connectors in tetragonal crystalline lattices are 12-mers complies well with the findings in other phage systems, although Tsuprun *et al.* (1994) observed 13-meric phi29 connectors both in hexagonal lattices and as single particles. The arguments in favor of our observed connectors being 12-mers are:

(i) In the map calculated in p1, i.e., without any symmetry imposed, 12 protrusions appear along the outer periphery. Partial overlap of the domains of one connector with its neighbor may explain the different densities in different peripheral domains, in addition to some degree of flexibility of each individual domain.

(ii) The fact that the connectors form a p4 lattice also counts in favor of a dodecamer.

(iii) The analysis of the rotational symmetry is clearly in favor of a 12- rather than a 13-fold symmetry.

(iv) Upon disruption of virions, the connectors remain complexed with the tails (Rishovd *et al.*, 1994). This indicates a higher degree of symmetry match with the 6-fold tails than with the 5-fold capsid vertices.

A preliminary rotational analysis of single particles (data not shown) suggests that both 12- and 13-mers are present in the sample. Thus, 12-mers may be selected in the crys-

TABLE 1  
Bacterial and Phage Strains

Designation	Relevant characteristics	Reference
Bacteria		
C1a	Wild type	Sasaki and Bertani (1965)
C-317	C1a(PWamL <sub>9</sub> )	Sunshine <i>et al.</i> (1971)
C-322	C1a(P2 <i>amp</i> <sub>137</sub> )	Sunshine <i>et al.</i> (1971)
C-373	C1a(P2 <i>Ig tsV</i> <sub>199</sub> )	Haggård-Ljungquist <i>et al.</i> (1995)
C-1512	C1a(P2 <i>tsM</i> <sub>52</sub> )	Lindahl (1969)
C-1592	C1a(P2 <i>cox3</i> )	Lindahl and Sunshine (1972)
C1a(pRG1 + pNL93Q)	C1a derivative overproducing gpQ	Linderoth <i>et al.</i> (1991)
Phages		
P4 <i>vir1</i>	Immunity insensitive	Lindqvist and Six (1971)

tallization process. The angle between subunits is 30° in a 12-mer in contrast to 27.7° in a 13-mer. Presumably, this 2.3° difference can be accounted for by the interacting subunits, at least in the nonbiological situation when the connector protein is produced in large amounts in the absence of other phage proteins. Although it is conceivable that the assembly of the connector is strictly controlled to ensure the production of only one type of oligomer, so far no control mechanism has been proposed or described in any phage system. Also, the connector protein is in many cases produced in large excess, by far exceeding the amount actually incorporated into virions. Thus, it is possible that the flexibility of the subunits, being essential for proper connector function (in capsid assembly, DNA packaging, connection of a tail, and DNA ejection) render the production of one oligomeric type exclusively too costly. Capsid protein monomers/oligomers would then have to select the correct connector oligomer with which to assemble procapsids.

Our genetic experiments demonstrate that the cleavage of the connector protein depends on the terminase subunit gpP. The procapsids accumulating during a P4 infection of lysogens defective in gene *P* contain uncleaved connector protein only. In contrast, cells accumulating capsids after DNA packaging, due to the absence of capsid completion protein gpL, contain cleaved gpQ comparable to the wild-type situation. We cannot exclude the possibility that the processing of gpQ may be a function of gpP separated from its role as a terminase subunit. However, we favor the possibility that the processing of the connector is an integral part of the DNA packaging process. The observation of relatively small amounts of Q\* in the M<sup>-</sup> situation might reflect leakiness of the temperature-sensitive allele used, or that gpP exerts its function on gpQ without depending on gpM. In a previous paper (Rishovd *et al.*, 1994) we noted the similarity of the amino termini of gpQ, phage phi29 gp10 (the sequence responsible for the DNA binding properties of the connector protein (Donate *et al.*, 1992)), and murine polyoma virus VP1 (a capsid protein, the amino terminus of which has been shown to bind DNA

(Chang *et al.*, 1993)). Based on this we suggested a possible role for this highly basic amino-terminal fragment of gpQ in DNA binding. The finding that this fragment is removed from the connector during DNA packaging substantiates this suggestion. Conceivably, the gpQ amino terminus may bind DNA in the initiation of the DNA packaging process. Cleavage may be necessary for the process to proceed, and the cleaved fragment may be released or remain complexed to DNA in the capsid. Alternatively, the amino terminus may bind DNA nonspecifically throughout the packaging process, and the cleavage may be necessary to complete the process. Even in this scenario the cleaved fragment may enter the capsid along with the DNA. This nonspecific binding of DNA by probably 12 amino termini in a single connector may constitute a molecular guide for the entry of DNA into the capsid. This scenario is in line with the suggestion of Dube *et al.* (1993) that the connector probably passively relieves stress in the packaged DNA molecule by rotation relative to the capsid (due to the symmetry mismatch) rather than participating actively as the motor for the packaging process.

The only other case of connector protein cleavage previously described is from phage λ. However, the mature λ virion contains both uncleaved and cleaved gpB (connector protein) (Hendrix and Casjens, 1975; Muri- aldo and Siminovitch, 1972) and any possible function of this cleavage reaction remains unknown.

## MATERIALS AND METHODS

### Bacterial strains and phages

The bacterial strains and phage stocks are described in Table 1. Stocks were produced as described in Rishovd and Lindqvist (1992), and phage virions were purified by isopycnic ultracentrifugation (200,000*g*, 16°C, 18 h) in a CsCl gradient (0.54 g/ml).

### Purification of gpQ

The gene *Q* product was purified from the strain C1a(pRG1+pNL93Q) (kindly provided by Nora Linderoth

and Richard Calendar). This strain expresses gene *O* from a T7 P<sub>A1</sub> promoter under the control of *lacO* (Linderoth *et al.*, 1991) after induction with 5 mM IPTG. The purification was performed as described in Rishovd *et al.* (1994). Protein concentrations were determined according to the Bio-Rad Protein Assay Kit.

### SDS–Page

A discontinuous Laemmli buffer system (Laemmli, 1970) was used together with the standard procedures for SDS–PAGE as described in Sambrook *et al.* (1989). Samples were prepared according to Rishovd and Lindqvist (1992).

### Immunodetection of proteins

After SDS–PAGE, the proteins were electroblotted at 400 mA for 1 h onto Immobilon P membranes (Millipore). Serum concentrations of about 1:15,000 in TBST/skim milk (20 mM Tris–Cl, pH 7.5, 500 mM NaCl, 0.05% Tween 20, with 5% skim milk added) were used after preincubation against *E. coli* extract (as described in Sambrook *et al.*, 1989). Secondary antibodies were biotinylated goat anti-rabbit IgG (Bio-Rad) linked by streptavidin to biotinylated horseradish peroxidase used according to the manufacturer's recommendations. The ECL system from Amersham was used for detection of the antigens.

### Infection experiments

Cells harboring P2 late gene mutant prophages were grown in LB medium (supplemented with 0.1% glucose, 2.0 mM MgSO<sub>4</sub> and 0.5 mM CaCl<sub>2</sub>) to OD<sub>600</sub> = 0.3 at 37°C (at 42°C when the prophage mutant was temperature sensitive) and infected with P4*vir1* at m.o.i. = 1–2. Incubation was allowed to continue until lysis, and 1-ml samples were collected every 10 min during the infection. The cells of each sample were pelleted in an Eppendorf table centrifuge (13,000 rpm, 30 s), the supernatant was removed, and the cell pellets were frozen immediately in liquid N<sub>2</sub>.

### Two-dimensional (2D) crystallization and electron microscopy

2D crystals of the connector protein were grown using a procedure based on the method described by Holzenburg (1988) with the following modifications: (i) 6  $\mu$ l of a 40% saturated ammonium sulfate solution, (ii) 1  $\mu$ l of 1.5 M Tris buffer (pH 8.8), and (iii) 1  $\mu$ l of purified gpQ (1 mg/ml) in 10 mM Tris–Cl, pH 7.5, were successively added to a 11- $\mu$ l droplet of distilled water, thoroughly mixed, and placed on a sheet of Parafilm. Subsequently, a carbon-coated copper grid (300 mesh) was placed on the top of the droplet and incubated for 5 min at 37°C. The grid was then transferred onto two droplets of Milli-Q water, quickly blotted to remove excess liquid, stained on

a droplet of an aqueous solution of uranyl acetate (1% w/v, pH 4.5) for 30 s, and blotted dry with the grid perpendicular to the filter paper. Grids were examined in a Philips CM12 transmission electron microscope operated at an accelerating voltage of 120 kV. Electron micrographs were recorded at calibrated magnifications (35,000 and 60,000 $\times$ ) on Kodak Electron Image Plate 4486 using electron doses 1000 e<sup>-</sup>/nm<sup>2</sup>.

### Image analysis and processing

Electron micrographs were assessed by optical diffraction using an optical bench. Using a Joyce-Loebel rotating drum microdensitometer, selected films were digitized at 25- $\mu$ m increments corresponding to pixel sizes of 7.1 Å or 4.2 Å at the specimen level, and imported into the PC-based crystallographic image processing software package CRISP (Hovmøller, 1992). Crystalline areas suitable for further analysis were boxed off, and numerical diffraction patterns were calculated, analyzed, and indexed. A resolution cutoff frequency of 0.04 Å<sup>-1</sup> was used throughout this work. Amplitudes and phases were first individually refined for each crystalline area and Fourier projection maps were calculated. The handedness was checked in each map, and for the final map three individual data sets displaying identical handedness were merged.

Single particles, observed as individual connectors in noncrystalline areas of the sample, were analyzed for their rotational symmetry using both analogue and digital methods. The digital method involved rotating molecules at desired angular increments and calculating the correlation between rotated and unrotated density distributions (calculation of the rotational power spectrum) and was carried out using the program 'power' (Dr. N. M. Glykos, IMBB, FORTH, Heraklion, Greece) run on a VAX workstation 4000/60 under VMS. The analogue method for analysis of the symmetry involved rotational integration carried out as described by Markham *et al.* (1963).

### ACKNOWLEDGMENTS

This work was in part supported by a post-doctorate stipend from The Faculty of Mathematics and Natural Science at the University of Oslo and by a grant from The Norwegian Research Council. We acknowledge financial support by The Academic Development Fund of the University of Leeds and the Leeds Center for Molecular Recognition in Biological Sciences. We also thank Dr. P. Tavares for his critical reading of the manuscript and for constructive comments.

### REFERENCES

- Bazinet, C., Benbasat, J., King, J., Carazo, J. M., and Carrascosa, J. L. (1988). Purification and organization of the gene 1 portal protein required for phage P22 DNA packaging. *Biochemistry* **27**, 1849–1856.
- Bazinet, C., and King, J. (1985). The DNA translocating vertex of dsDNA bacteriophages. *Annu. Rev. Microbiol.* **39**, 109–129.
- Black, L. W. (1988). "The Bacteriophages" (R. Calendar, Ed.), 2nd ed., Vol. 2, pp. 321–373. Plenum, New York.
- Carazo, J. M., Donate, L. E., Herranz, L., Secilla, J. P., and Carrascosa,

- J. L. (1986). Three-dimensional reconstruction of the connector of bacteriophage Phi29 at 1.8 nm resolution. *J. Mol. Biol.* **192**, 853–867.
- Carazo, J. M., Santisteban, A., and Carrascosa, J. L. (1985). Three-dimensional reconstruction of bacteriophage phi29 neck particles at 2.2 nm resolution. *J. Mol. Biol.* **183**, 79–88.
- Carrascosa, J. L., Carazo, J. M., Ibanez, C., and Santisteban, A. (1985). Structure of phage phi29 connector protein assembled *in vivo*. *Virology* **141**, 190–200.
- Chang, D., Cai, X., and Consigli, R. A. (1993). Characterization of the DNA binding properties of polyomavirus capsid proteins. *J. Virol.* **67**, 6327–6331.
- Dokland, T., Lindqvist, B. H., and Fuller, S. D. (1992). Image reconstruction from cryo-electron micrographs reveals the morphopoietic mechanism in the P2-P4 bacteriophage system. *EMBO J.* **11**(3), 839–846.
- Dokland, T., Isaksen, M. L., Fuller, S. D., and Lindqvist, B. H. (1993). Capsid localization of the bacteriophage P4 Psiu protein. *Virology* **194**, 682–687.
- Donate, L. E., Herranz, L., Secilla, J. P., Carazo, J. M., Fujisawa, H., and Carrascosa, J. L. (1988). Bacteriophage T3 connector: three-dimensional structure and comparison with other viral head-tail connecting regions. *J. Mol. Biol.* **201**, 91–100.
- Donate, L. E., Valpuesta, J. M., Rocher, A., Mendez, E., Rojo, F., Salas, M., and Carrascosa, J. L. (1992). Role of the amino-terminal domain of bacteriophage Phi29 connector in DNA binding and packaging. *J. Biol. Chem.* **267**(15), 10919–10924.
- Driedonks, R. A., and Caldentey, J. (1983). Gene 20 product of bacteriophage T4. II. Its structural organization in prehead and bacteriophage. *J. Mol. Biol.* **166**, 341–360.
- Driedonks, R. A., Engel, A., tenHeggeler, B., and van Driel, R. (1981). Gene 20 product of bacteriophage T4. Its purification and structure. *J. Mol. Biol.* **152**, 641–662.
- Dube, P., Tavares, P., Lurz, R., and van Heel, M. (1993). The portal protein of bacteriophage SPP1: A DNA pump with 13-fold symmetry. *EMBO J.* **12**(4), 1303–1309.
- Haggård-Ljungquist, E., Jacobsen, E., Rishovd, S., Six, E. W., Nilssen, Ø., Sunshine, M. G., Lindqvist, B. H., Kim, K.-J., Barreiro, V., Koonin, E. V., and Calendar, R. (1995). Bacteriophage P2: Genes involved in base-plate assembly. *Virology* **213**, 109–121.
- Hendrix, R., and Casjens, S. (1975). Assembly of bacteriophage lambda heads: Protein processing and its genetic control in petit lambda assembly. *J. Mol. Biol.* **91**, 187–199.
- Holzenburg, A. (1988). Preparation of two-dimensional arrays of soluble proteins as demonstrated for bacterial d-ribulose-1,5-bisphosphate carboxylase/oxygenase. *Methods Microbiol.* **20**, 341–356.
- Holzenburg, A., and Mayer, F. (1989). d-ribulose-1,5-bisphosphate carboxylase/oxygenase: Function-dependent structural changes. *Electron Microsc. Rev.* **2**, 139–169.
- Hovmøller, S. (1992). CRISP: Crystallographic image processing on a personal computer. *Ultramicroscopy* **41**, 121–135.
- Ibanez, C., Garcia, J. A., Carrascosa, J. L., and Salas, M. (1984). Overproduction and purification of the connector protein of *Bacillus subtilis* phage Phi29. *Nucleic Acids Res.* **12**(5), 2351–2365.
- Kochan, J., Carrascosa, J. L., and Murialdo, H. (1984). Bacteriophage lambda preconnectors. Purification and structure. *J. Mol. Biol.* **174**, 433–447.
- Laemmli, U. K. (1970). Cleavage of the structural proteins during the assembly of the head of bacteriophage T4. *Nature* **227**, 680–685.
- Lindahl, G. (1969). Genetic map of bacteriophage P2. *Virology* **39**, 839–860.
- Lindahl, G. (1971). On the control of transcription in bacteriophage P2. *Virology* **46**, 620–633.
- Lindahl, G. and Sunshine, M. (1972). Excision defective mutants of bacteriophage P2. *Virology* **49**, 180–187.
- Linderoth, N. A., Ziermann, R., Haggård-Ljungquist, E., Christie, G. E., and Calendar, R. (1991). Nucleotide sequence of the DNA packaging and capsid synthesis genes of bacteriophage P2. *Nucleic Acids Res.* **19**(25), 7207–7214.
- Lindqvist, B. H., and Six, E. W. (1971). Replication of bacteriophage P4 DNA in a nonlysogenic host. *Virology* **43**, 1–7.
- Markham, R., Frey, S., and Hils, G. J. (1963). Methods for the enhancement of image details and accentuation of structure in electron microscopy. *Virology* **20**, 88–102.
- Marvik, O. J., Dokland, T., Nøklng, R. H., Jacobsen, E., Larsen, T., and Lindqvist, B. H. (1995). The capsid size-determining protein Sid forms an external scaffold on phage P4 procapsids. *J. Mol. Biol.* **251**, 59–75.
- Murialdo, H., and Siminovitch, L. (1972). The morphogenesis of phage lambda. IV. Identification of gene products and control of the expression of the morphogenetic information. *Virology* **48**, 785–823.
- Pruss, G. J., and Calendar, R. (1978). Maturation of bacteriophage P2 DNA. *Virology* **86**, 454–467.
- Rishovd, S. (1993). "Bacteriophage P2 and P4 Morphogenesis: Identification and Characterization of Capsid Components." Ph.D. thesis, Univ. Of Oslo.
- Rishovd, S., and Lindqvist, B. H. (1992). Bacteriophage P2 and P4 morphogenesis: protein processing and capsid size determination. *Virology* **187**, 548–554.
- Rishovd, S., Marvik, O. J., Jacobsen, E., and Lindqvist, B. H. (1994). Bacteriophage P2 and P4 morphogenesis: Identification and characterization of the portal protein. *Virology* **200**, 744–751.
- Sambrook, J., Fritsch, E. F., and Maniatis, T. (1989). "Molecular Cloning: A Laboratory Manual.", Cold Spring Harbor Press, Cold Spring Harbor, NY.
- Sasaki, I., and Bertani, G. (1965). Growth abnormalities in Hfr derivatives of *Escherichia coli* strain C. *J. Gen. Microbiol.* **40**, 365–376.
- Tsuprun, V., Anderson, D., and Egelman, E. H. (1994). The bacteriophage phi29 head-tail connector shows 13-fold symmetry in both hexagonally packed arrays and as single particles. *Biophys. J.* **66**, 2139–2150.
- Valpuesta, J. M., Fujisawa, H., Marco, S., Carazo, J. M., and Carrascosa, J. L. (1992). Three-dimensional structure of T3 connector purified from overexpressing bacteria. *J. Mol. Biol.* **224**, 103–112.
- Valpuesta, J. M., and Carrascosa, J. L. (1994). Structure of viral connectors and their function in bacteriophage assembly and DNA packaging. *Quart. Rev. Biophys.* **27**, 107–155.
- Zachary, A., and Black, L. W. (1992). Isolation and characterization of a portal protein-DNA complex from dsDNA bacteriophage. *Intervirology* **33**, 6–16.